

Systematic analysis of barrier-forming FG hydrogels from *Xenopus* nuclear pore complexes

Aksana A Labokha¹, Sabine Gradmann²,
Steffen Frey¹, Bastian B Hülsmann¹,
Henning Urlaub^{3,4}, Marc Baldus²
and Dirk Görlich^{1,*}

¹Abteilung Zelluläre Logistik, Max-Planck-Institut für biophysikalische Chemie, Göttingen, Germany, ²Bijvoet Center for Biomolecular Research, Utrecht University, Utrecht, The Netherlands, ³Bioanalytische Massenspektrometrie, Max-Planck-Institut für biophysikalische Chemie, Göttingen, Germany and ⁴Bioanalytik, Abteilung Klinische Chemie Universitätsmedizin Göttingen, Göttingen, Germany

Nuclear pore complexes (NPCs) control the traffic between cell nucleus and cytoplasm. While facilitating translocation of nuclear transport receptors (NTRs) and NTR·cargo complexes, they suppress passive passage of macromolecules ≥ 30 kDa. Previously, we reconstituted the NPC barrier as hydrogels comprising *S. cerevisiae* FG domains. We now studied FG domains from 10 *Xenopus* nucleoporins and found that all of them form hydrogels. Related domains with low FG motif density also substantially contribute to the NPC's hydrogel mass. We characterized all these hydrogels and observed the strictest sieving effect for the Nup98-derived hydrogel. It fully blocks entry of GFP-sized inert objects, permits facilitated entry of the small NTR NTF2, but arrests importin β -type NTRs at its surface. O-GlcNAc modification of the Nup98 FG domain prevented this arrest and allowed also large NTR·cargo complexes to enter. Solid-state NMR spectroscopy revealed that the O-GlcNAc-modified Nup98 gel lacks amyloid-like β -structures that dominate the rigid regions in the *S. cerevisiae* Nsp1 FG hydrogel. This suggests that FG hydrogels can assemble through different structural principles and yet acquire the same NPC-like permeability.

The EMBO Journal (2013) 32, 204–218. doi:10.1038/emboj.2012.302; Published online 30 November 2012

Subject Categories: membranes & transport; proteins

Keywords: exportin; FG hydrogel; importin; nuclear pore complex; O-glycosylation

Introduction

Nuclear pore complexes (NPCs) connect the nuclear interior with the cytoplasm and control the exchange between the two compartments. They are built from nucleoporins (Nups; reviewed in Brohawn *et al*, 2009 and Hetzer and Wentz, 2009) and are equipped with a sieve-like barrier that is freely permeable for small molecules, but becomes increasingly

restrictive as inert mobile species approach or exceed 5 nm in diameter (Mohr *et al*, 2009). This limit corresponds to a mass of ≈ 30 kDa for spherical proteins. Nuclear transport receptors (NTRs) can overcome this size limit and transfer even very large cargoes across NPCs. Such 'facilitated translocation' is used to supply nuclei with proteins and the cytoplasm with nuclear products such as ribosomes or mRNAs.

Importin β -type receptors represent the largest class of NTRs and include importins as well as exportins (reviewed in Fried and Kutay, 2003). The RanGTP gradient model (Görlich *et al*, 1996; Izaurrealde *et al*, 1997) provides an explanation for the directionality of the corresponding transport pathways: Importins recruit cargo at low RanGTP levels in the cytoplasm, release their cargo upon RanGTP-binding into the nucleus, and return RanGTP-bound to the cytoplasm. There, GTP hydrolysis triggers dissociation of the importin·RanGTP complex and allows the importin to bind a next cargo molecule. A prototypical example is importin β itself (Imp β ; Chi *et al*, 1995; Görlich *et al*, 1995; Imamoto *et al*, 1995). It binds import cargoes either directly or through an adaptor such as importin α (Imp α).

Exportins recruit cargoes inside nuclei together with RanGTP (reviewed by Güttler and Görlich, 2011). Examples are CAS/exportin 2, which exports Imp α , or CRM1 that exports many substrates, including ribosomal subunits. Another NTR category is exemplified by the homodimeric RanGDP importer NTF2, which is structurally unrelated to Imp β (Bullock *et al*, 1996; Ribbeck *et al*, 1998).

Facilitated translocation is remarkably efficient. A single NPC can accommodate ≈ 1000 transport events per second (Ribbeck and Görlich, 2001) and needs as little as ≈ 10 ms to translocate an Imp β ·cargo complex from the cytoplasmic to the nuclear side of the pore (Yang *et al*, 2004; Kubitschek *et al*, 2005). These numbers imply that NPCs are able to translocate numerous objects simultaneously. Facilitated translocation is not directly coupled to an input of metabolic energy (Schwoebel *et al*, 1998; Englmeier *et al*, 1999; Ribbeck *et al*, 1999). Instead, it is primarily based on a higher permeability of NPCs for NTRs as compared to inert molecules; and it is the cooperation of importins or exportins with the RanGTPase system that renders NPCs into active and highly efficient cargo pumps (Görlich *et al*, 2003).

Non-globular nucleoporin FG domains are central for the function of the NPC barrier (Hurt, 1988; Strawn *et al*, 2004; Patel *et al*, 2007; Hülsmann *et al*, 2012). Their name derives from the frequent occurrence of Phenylalanine-Glycine (FG) dipeptides. They are typically several 100 residues long and comprise up to 50 FG, FxFG or GLFG motifs separated by spacers of rather variable sequence. For the sake of simplicity, these motifs are here collectively referred to as FG motifs. Metazoan NPCs contain several FG domains with multiple serine and threonine residues being modified with single O-linked β -N-acetylglucosamine (O-GlcNAc) moieties (Finlay *et al*, 1987; Hanover *et al*, 1987; Holt *et al*, 1987; Onischenko *et al*, 2005). The function of this modification of FG domains is still unknown.

*Corresponding author. Abteilung Zelluläre Logistik, Max-Planck-Institut für biophysikalische Chemie, Am Fassberg 11, Göttingen 37077, Germany.
Tel.: +49 551 201 2401; Fax: +49 551 201 2407;
E-mail: goerlich@mpibpc.mpg.de

Received: 14 September 2012; accepted: 29 October 2012; published online: 30 November 2012

FG motifs bind NTRs during facilitated translocation (Iovine *et al.*, 1995; Rexach and Blobel, 1995; Bayliss *et al.*, 1999; Morrison *et al.*, 2003). How the FG·NTR interaction promotes NPC passage is, however, surprisingly difficult to answer. In fact, one would expect that a mere binding causes retention of NTRs and therefore slows down their passage. Also, such a simple binding cannot explain how inert material is excluded from passage.

To resolve this paradox, several models have been proposed. The ‘virtual gate’ model (Rout *et al.*, 2003) assumes that brushes of FG domains repel inert material and that NTRs overcome this barrier by binding to the domains. The ‘selective phase’ model (Ribbeck and Görlich, 2001) attributes an additional essential property to the barrier-forming FG domains, namely cohesiveness. It assumes that cohesive FG domains multivalently interact with each other and form a sieve-like hydrogel, the selective phase. The mesh size sets an upper size limit for unhindered NPC passage of inert material. According to the model, binding of an NTR to an FG motif disengages the corresponding repeat-repeat contact (Ribbeck and Görlich, 2001; Kustanovich and Rabin, 2004). NTRs can thus ‘melt’ through a dense FG hydrogel. The model is supported by the observations that the yeast *S. cerevisiae* (sc) contains several highly cohesive FG domains (Frey *et al.*, 2006; Frey and Görlich, 2007, 2009; Patel *et al.*, 2007; Yamada *et al.*, 2010), and that the FG domains from scNsp1p, the fused FG domains from scNup49p and scNup57p, or the human Nup153 FG domain indeed form FG hydrogels that display permeability properties very similar to authentic NPCs (Frey *et al.*, 2006; Frey and Görlich, 2007, 2009; Milles and Lemke, 2011). That is, they exclude inert macromolecules >5 nm, but allow an up to 20 000 times faster influx of the same macromolecule bound to an NTR. The rates of intragel diffusion are also consistent with the observed NPC transit times being in the 10 ms range (Yang *et al.*, 2004; Kubitschek *et al.*, 2005).

Analysis of the scNsp1 FG domain revealed that hydrophobic as well as hydrophilic interactions contribute to inter repeat cohesion (Frey *et al.*, 2006; Ader *et al.*, 2010). Mutating the hydrophobic residues (which are mainly phenylalanines) to serines abolishes gel formation. The N-terminal part of the domain (residues 1–175) is extremely cohesive and comprises inter FG spacers that are very rich in Asn, Gln and Thr. Solid-state NMR (ssNMR) revealed that these spacers engage in interchain β -sheets (Ader *et al.*, 2010)—similar to those found in NQ-rich amyloids (Eanes and Glenner, 1968; Balbirnie *et al.*, 2001). NQ-rich spacers characterize also the very cohesive GLFG domains from *S. cerevisiae* Nup100p or Nup116p (Yamada *et al.*, 2010; Halfmann *et al.*, 2012). The C-terminal part of the scNsp1 FG domain (residues \approx 274–601) is rather non-cohesive, apparently because the inter FG spacers are dominated by charged residues that counteract inter FG cohesion (Ader *et al.*, 2010; Yamada *et al.*, 2010). It is, however, adhesive in the sense that it (weakly) binds to and greatly improves the selectivity of the NQ-rich scNsp1^{1–175} FG hydrogel (Ader *et al.*, 2010).

If inter FG repeat cohesion was generally relevant for NPC function, then also eukaryotes other than *S. cerevisiae* should rely on this principle. We decided to test this prediction exhaustively for the Nups from the frog *Xenopus* and noticed similarities but also remarkable differences to yeast. *Xenopus* lacks NQ-rich inter FG spacers; nevertheless, we found all major FG domains to be cohesive and to form FG hydrogels.

We also characterized additional nucleoporin ‘FG-like’ domains representing low complexity sequences that are related to FG domains but contain only few or no FG motifs. We observed that they form hydrogels as well and might therefore substantially contribute to the NPC’s cohesive mass. Of all gels analysed, the O-GlcNAc-modified Nup98 FG hydrogel was the most selective, that is, it discriminated best between inert macromolecules and the tested spectrum of NTRs and NTR·cargo complexes. ssNMR revealed that this type of gel is devoid of β -structures, which is in striking contrast to the already-mentioned scNsp1 FG hydrogel. This suggests that FG hydrogel-based barriers can assemble through different structural principles and yet gain a very similar, NPC-like, selectivity.

Results

All *Xenopus* FG domains are cohesive and form FG hydrogels

Amyloid-like, intermolecular β -sheets between NQ-rich sequences are dominating structural elements in the hydrogel formed by the FG domain from *S. cerevisiae* Nsp1p (Ader *et al.*, 2010; Petri *et al.*, 2012). This coincides with a high NQ content (\approx 27%; Table I) of the most cohesive part of this domain (scNsp1^{1–175}) and of other highly cohesive yeast FG domains, such as those from scNup100p or scNup116p (Ader *et al.*, 2010; Yamada *et al.*, 2010; Halfmann *et al.*, 2012). This could suggest that NQ-rich inter FG spacers are required for any hydrogel-based NPC permeability barrier. The NQ content of *Xenopus* FG domains is, however, low (average: 9.6%, range: 5.8–12%; Table I) and close to the average of globular proteins from the PDB database (7.7%). This raised the questions if *Xenopus* FG domains are cohesive and if *Xenopus* NPCs actually rely on FG hydrogels for maintaining their permeability barriers.

To address this issue, we analysed a comprehensive set of *Xenopus* FG domains (Supplementary Figure S1). We cloned and expressed FG domains from Nup358, Nup214, Nup153, Nup98, Nup62, Nup58, Nup54, Nup50, Pom121 and CG1 in *Escherichia coli*, purified them under conditions that prevent any premature cohesion, and concentrated them by lyophilization. We then dissolved the proteins in an aqueous buffer at a concentration of \approx 200 mg/ml, which approximates the expected FG repeat concentration in authentic NPCs. Strikingly, none of those protein solutions remained liquid. Instead, all FG domains formed gels (see Figures 1A, 2B and 3A for a selection of gel photographs). In the case of the Pom121 and Nup62 FG domains, the solutions jellified so rapidly that we could not dissolve the lyophilized proteins completely. We therefore retarded gelation by the addition of 0.5–2 M guanidinium hydrochloride.

Xenopus FG hydrogels deviate from the paradigm of NQ-rich amyloids

Of all the *Xenopus* FG domains, the one derived from Nup98 has still the highest NQ content (12%). We observed efficient hydrogel formation, however, also with a mutant lacking Asn and Gln altogether (Nup98 FG NQ \Rightarrow S; Figure 1A). It thus seems that *Xenopus* FG domains can form gels without the hydrophilic interaction potential of NQ-rich inter FG spacers. In this respect, it is remarkable that *Xenopus* FG domains are considerably more hydrophobic than the FG domains from yeast scNsp1p or scNup100p (Table I). Thus, while inter FG

Table I Composition of FG and FG-like domains from *Xenopus* and *S. cerevisiae*

Repeat domain	Residues	FG dipeptides per 100 residues	% N+Q	% T	% D+E+K+R	Mean hydrophobicity
<i>S.c.</i> Nsp1p FG	1-175	6.8	26.7	15.9	2.3	0.15
	274-601	5.2	6.7	4.6	34.8	-0.06
<i>S.c.</i> Nup100p FG	2-580	7.3	27.3	10.2	4.1	0.19
<i>X.l.</i> Nup214 FG	1615-2033	8.8	8.8	9.5	2.4	0.36
	FG-like-1	443-690	0.8	8.9	10.1	0.40
	FG-like-2	1220-1614	0.8	6.6	12.9	0.37
<i>X.t.</i> Nup153 FG	885-1525	5.0	8.4	10.9	9.7	0.30
	885-1127	4.5	5.4	11.9	21.0	0.20
	1128-1525	5.3	10.3	10.3	2.5	0.36
<i>X.l.</i> Nup62 FG	2-352	3.1	7.1	17.8	1.7	0.41
<i>X.l.</i> Nup58 FG	2-72, 511-598	6.9	7.5	15.0	4.4	0.34
	FG&FG-like	2-259, 511-598	3.2	8.9	15.6	2.9
<i>X.l.</i> Nup54 FG	2-94	10.7	6.5	28.0	2.2	0.41
	FG&FG-like	2-139	7.3	11.5	25.4	1.5
<i>X.t.</i> Nup98 FG ^{AGLEBS}	1-485	9.6	12.0	20.4	2.3	0.37
<i>X.l.</i> Pom121 FG	571-1050	1.7	10.0	15.0	7.9	0.37
<i>X.l.</i> Nup50 FG	68-285	3.7	7.4	9.8	12.9	0.29
<i>X.l.</i> CG1 FG	257-411	5.8	5.8	11.6	5.2	0.40
<i>X.t.</i> Nup358 FG	Combined	2.5	10.0	7.0	25.0	0.22
	1625-1837	2.4	12.2	6.1	24.4	0.19
	1967-2119	0.7	7.2	9.2	30.1	0.16
	2315-2431	3.4	8.6	6.8	19.7	0.30
	2572-2725	2.0	4.6	4.6	27.3	0.20
PDB average		0.3	7.7	5.5	22.8	0.37

S. c., *Saccharomyces cerevisiae*; *X. l.*, *Xenopus laevis*; *X. t.*, *Xenopus tropicalis*. The mean hydrophobicity was calculated according to the scale of Fauchere and Pliska (1983). The scale is based on partitioning of *N*-acetyl-amino-acid amides between 1-octanol and water at neutral pH; it ranges between +2.25 for polyW and -1.01 for polyR. The combined Nup358 FG domain is a fusion of nine FG subdomains comprising following residues: 1095-1180, 1307-1345, 1374-1469, 1504-1528, 1558-1595, 1625-1837, 1967-2119, 2315-2431 and 2572-2725.

cohesion in *S. cerevisiae* relies on both, hydrophobic and hydrophilic interactions (Ader *et al.*, 2010), hydrogel formation in vertebrates appears to have a stronger hydrophobic basis (see also below). It is also remarkable that even the most highly charged *Xenopus* FG domains, such as the combined Nup358 FG domains with 25% charged residues, formed a hydrogel (Table I and Figure 1A and C).

The Nup98 FG domain forms the FG hydrogel with the strictest sieving effect

In a next step, we explored the permeability properties of all 10 *Xenopus* FG hydrogels. Specifically, we tested their ability to restrict the passage of inert molecules and to allow

facilitated translocation of NTRs. For that, we formed the gels on microscope slides, equilibrated them in assay buffer, added fluorescent probes to the buffer reservoir, and measured the entry of these probes into the hydrogels by confocal laser-scanning microscopy. The first set of probes included mCherry (Shaner *et al.*, 2004) as an ≈ 26 kDa inert molecule and Alexa488-labelled NTF2 as a small (29 kDa) NTR (Figure 1B).

This probing revealed the Nup98 gel as the most selective barrier. The gel fully excluded mCherry, that is, the gel/buffer partition coefficient for mCherry was essentially zero. The Nup98 gel is thus more restrictive than authentic NPCs, which allow GFP-sized molecules to pass at clearly detectable

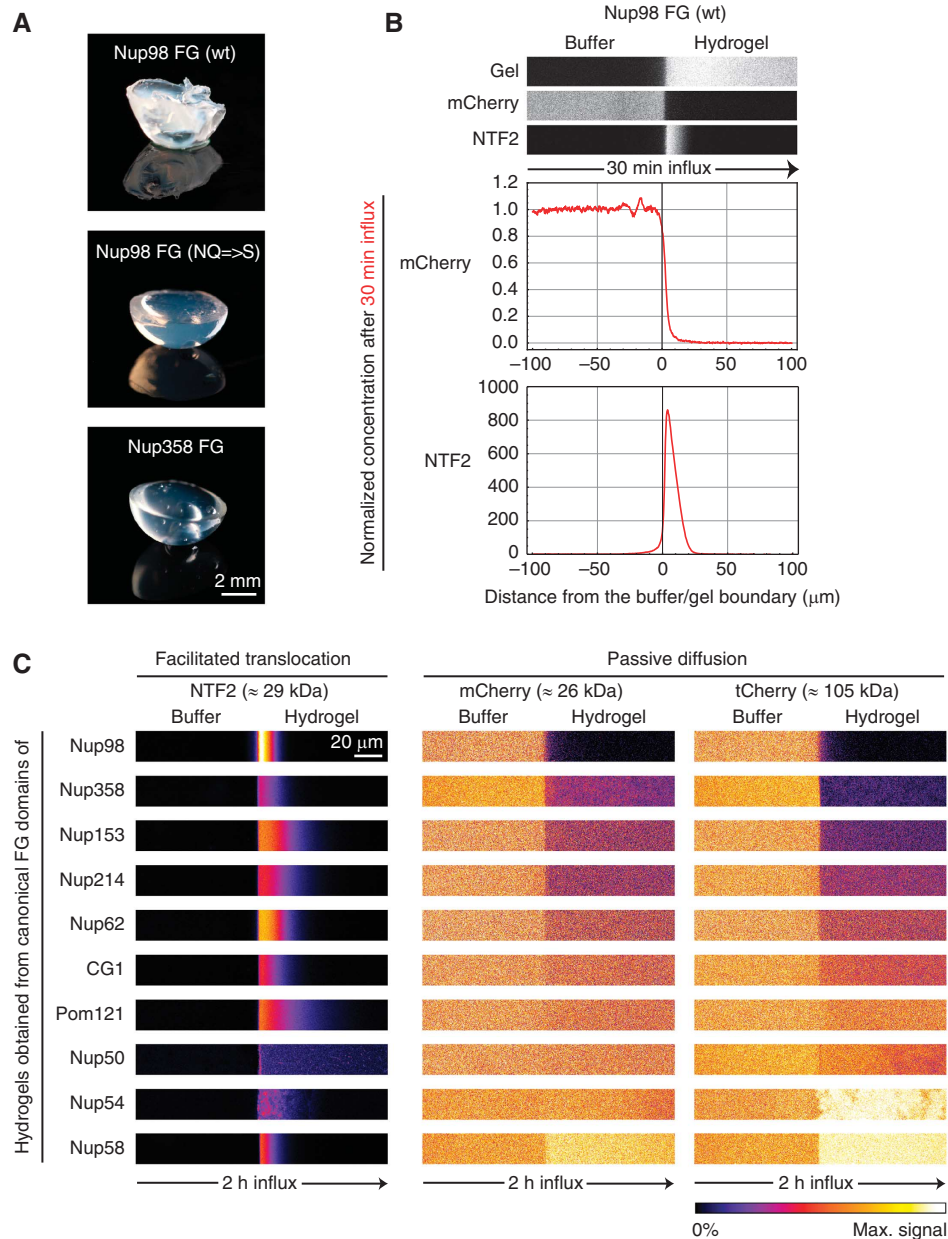


Figure 1 Selectivity properties of hydrogels derived from *Xenopus* FG domains. **(A)** Macroscopic pictures of Nup98 (wild type; wt), Nup98 (NQ \Rightarrow S mutant) and Nup358 FG hydrogels. The used Nup358 domain combines all nine FG subdomains of the protein (Table I). Gels were formed on parafilm, inverted and photographed. **(B)** Simultaneous influx of mCherry and NTF2-A1488 into a Nup98 FG (wt) hydrogel measured after 30 min by confocal laser-scanning microscopy. The far-red labelled hydrogel was detected after excitation at 633 nm, mCherry at 561 nm and Alexa488-labelled NTF2 at 488 nm. Arrow illustrates direction of influx. Concentration profiles of mCherry and NTF2 across the buffer/gel boundary are also shown. For normalization, free NTF2 and mCherry concentrations in the buffer had been set to 1. **(C)** Two-hour-influx of NTF2, mCherry and tCherry into 10 different *Xenopus* FG hydrogels (for sequences of used domains, see Supplementary Figure S1 and Supplementary Table S1). False-coloured fluorescent signals illustrate partitioning of mobile species between buffer and gels. Note that the isolated FG domains of Nup54 and Nup58 show non-specific binding to tCherry (see also Figure 4).

rates (Mohr *et al*, 2009). Nevertheless, NTF2 was able to enter the Nup98 gel efficiently, reaching within 30 min a partition coefficient of nearly 1000. Importantly, NTF2 did not remain stuck at the gel surface, but moved deep into the gel, on average $10\mu\text{m}$ during 30 min incubation. At such diffusion rate, it would take ≈ 50 ms to cross a 50-nm thick NPC barrier. This is ≈ 10 -fold slower than expected for passing an authentic NPCs (Kubitscheck *et al*, 2005), but consistent with the observation that the Nup98 FG hydrogel forms an extraordinary tight barrier (see below).

Except for the Nup50 gel, we found that all other *Xenopus* FG hydrogels allowed a similarly efficient NTF2 influx (Figure 1C). These gels differed, however, clearly from the Nup98 gel by a less efficient exclusion of inert probes. The Nup153, Nup214 and Nup358 FG hydrogels displayed an intermediate efficiency as a passive barrier: they were rather permeable towards mCherry, but visibly restrictive towards the tetramerized (105 kDa) tCherry version. The Pom121 and Nup50 FG hydrogels were not only highly permeable for mCherry, but also for tCherry. The Nup54 and Nup58 FG

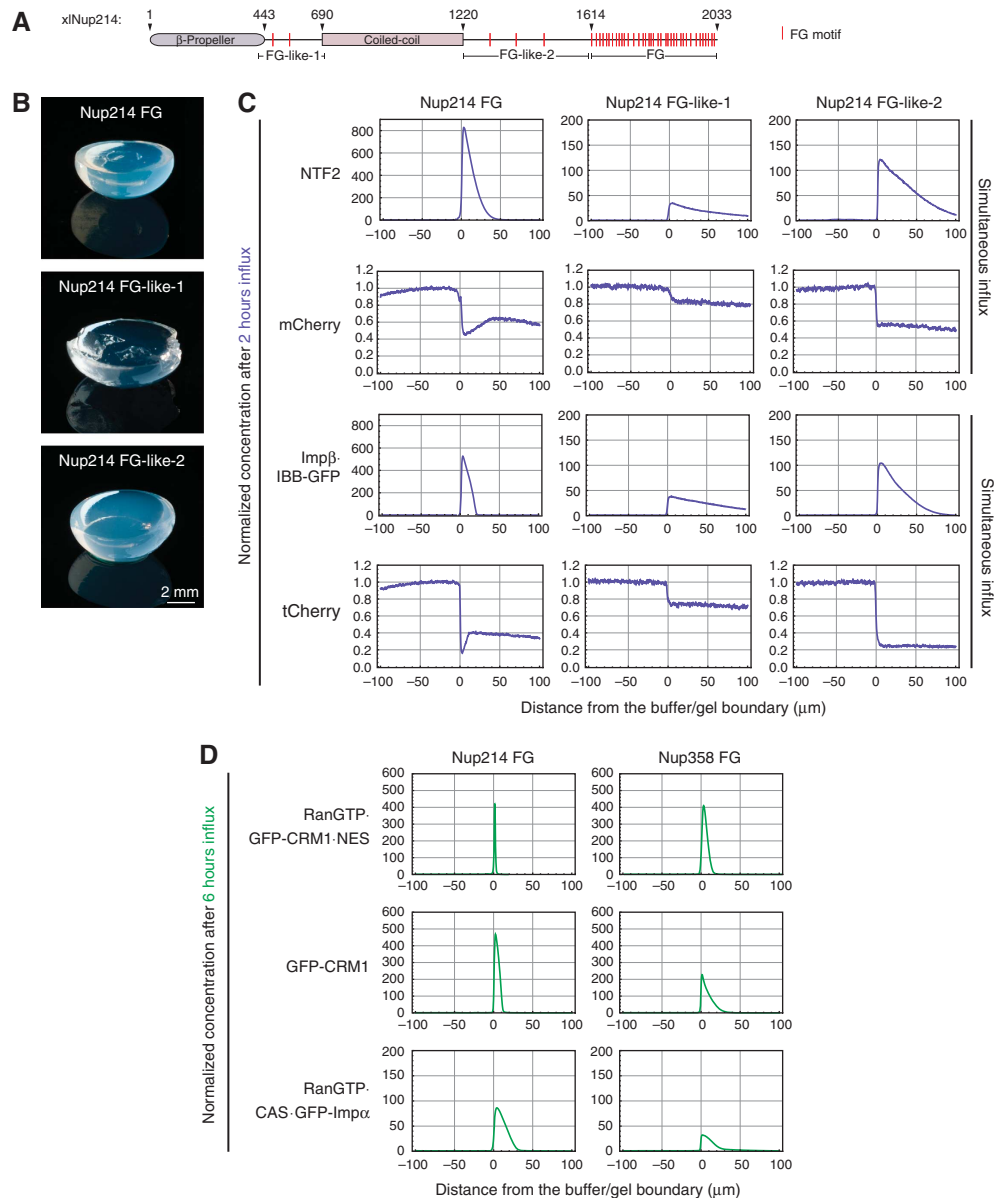


Figure 2 Selectivity properties of Nup214 hydrogels. **(A)** Domain organization of *Xenopus laevis* Nup214. Red strokes represent FG motifs. Nup214 contains a canonical FG domain ('FG') as well as two FG-like domains. **(B)** Photographs of indicated hydrogels. **(C)** Simultaneous influx of NTF2 and mCherry or of Imp β ·IBB-GFP and tCherry into indicated hydrogels (2 h time points). Permeation assays were performed as in Figure 1. Note the deviating scaling of NTF2 and Imp β ·IBB-GFP signals for the FG-like hydrogels. **(D)** Influx of RanGTP·GFP-CRM1·NES export complex into Nup214 hydrogels as compared to Nup358 FG hydrogels (6 h time points). Influx of free GFP-CRM1 and of a CAS export complex is shown as controls.

hydrogels even showed an enrichment of our (otherwise) inert probes, indicating a propensity for non-specific binding. This illustrates an interesting point, namely that it is not trivial that a gel, which comprises unfolded and rather hydrophobic domains, is well passivated against non-selective interactions with other proteins. We will come back to this important issue later on. Before, however, we will describe the FG hydrogels derived from Nup214, Nup358, Nup153, the Nup62·54·58 complex, and Nup98 in greater detail.

Nup214 contains three gel-forming FG subdomains

Nup214 is localized to the cytoplasmic side of NPCs, where it forms a subcomplex with Nup62 and Nup88 (Kraemer *et al*, 1994; Bastos *et al*, 1997; Fornerod *et al*, 1997). Nup214 comprises two globular domains: an N-terminal beta-propeller

binding the mRNA-export factor DDX19/Dbp5 (Weirich *et al*, 2004; von Moeller *et al*, 2009) as well as a coiled-coil domain, which presumably accounts for the interaction with Nup62 and Nup88, and which anchors the complex to the scaffold of the NPC (Bernad *et al*, 2006). Nup214 contains at its C-terminus the already-mentioned canonical FG domain, which comprises 419 residues, features a high density of FG motifs (one motif per 12 residues; Figure 2A; Supplementary Figure S1; Table I), and displays a similar degree of sequence conservation as the beta-propeller or the central coil-coiled region. As mentioned above, this canonical FG domain forms an FG hydrogel (Figures 1C and 2B).

Nup214 contains two additional domains with a predicted non-globular structure, namely a 248 residues long stretch connecting beta-propeller and coiled-coil as well as a 395-

residue long region preceding the canonical FG domain (Figure 2A). They only show a low level of inter species sequence conservation. Their low complexity amino-acid composition resembles canonical FG domains, but their FG motif density is very low (one motif per ≈ 125 residues, Table I). Nevertheless, these two ‘FG-like’ domains also formed hydrogels (Figure 2B). This implies that—assuming a copy number of eight per NPC—Nup214 alone may contribute nearly 1 MDa of hydrogel mass to an NPC.

The Nup214 FG hydrogel selectively stalls CRM1 export complexes

NTF2 and the Imp β ·IBB-GFP complex (≈ 120 kDa) entered all three Nup214-derived gels rapidly (Figure 2C). The canonical FG domain (which has the highest FG density) displayed, however, slower intragel diffusion and stronger NTR accumulation near the buffer-gel boundary. The diffusion of NTF2 and the Imp β ·cargo complex inside Nup214 FG-like gels was faster than in other *Xenopus* FG hydrogels tested. Remarkably, Nup214 FG-like-2 hydrogel suppressed influx of tCherry even more efficiently than the canonical domain resulting in a gel/buffer partition coefficient for tCherry being as low as 0.2.

It is known that loading of an FG hydrogel with NTRs counteracts the entry of inert macromolecules (Frey and Görlich, 2009). This effect is probably based on volume exclusion and on NTRs introducing additional cross-links into the gel. This effect was also clearly evident for the canonical FG hydrogel, but not for the FG-like ones, which probably reflects the fact that the canonical FG domain retains NTRs more strongly (Figure 2C, left column).

Previous reports indicated that Nup214 acts as a terminal binding site for CRM1 export complexes (Hutten and Kehlenbach, 2006). The interaction between such a RanGTP·CRM1·NES export complex with the gel of the

canonical Nup214 FG domain was indeed remarkable. The complex initially bound very rapidly to the gel, but showed hardly any movement away from the entry site (Figure 2D). This ‘traffic jam’ eventually also blocked further influx of complexes into the gel. The stalling at the buffer-gel boundary was very specific and was observed neither for free CRM1 nor for the RanGTP·CAS·Imp α export complex (Figure 2D). The selective retardation of a RanGTP·CRM1·cargo complex depended also on the choice of hydrogel (Supplementary Figure S2). In fact, the only other FG hydrogel that showed a similar effect was the one derived from Nup358/RanBP2, though retention of the RanGTP·CRM1·cargo complex was here not as strict (Figure 2D). Given that Nup358 and Nup214 probably are neighbours on the farthest cytoplasmic side of the NPC (Bernad *et al*, 2004), this is perhaps not just a pure coincidence.

The stalling indicates a very slow release of the NTR complex from specialized FG binding sites. In authentic NPCs, this could serve a substrate-channelling mechanism, where RanGTP·CRM1·cargo complexes are directly presented to the nearby Nup358/RanBP2-RanGAP system until GTP hydrolysis has occurred and the cargo has been released from the exportin into the cytoplasm. Such substrate channelling could improve the efficiency of these transport cycles, because it would prevent a backflow of RanGTP·CRM1·cargo complexes to the nucleus, and thus make export irreversible even before GTP hydrolysis has occurred. Also, this mechanism could allow cargo-free CRM1 to return to the nucleus without an intervening release into the bulk cytoplasm.

Hydrogels derived from highly charged FG domains

The Nup358 FG hydrogel is remarkable for its high content of charged residues (Table I), which is a feature that negatively correlates with the gel-forming propensity of *S. cerevisiae* FG

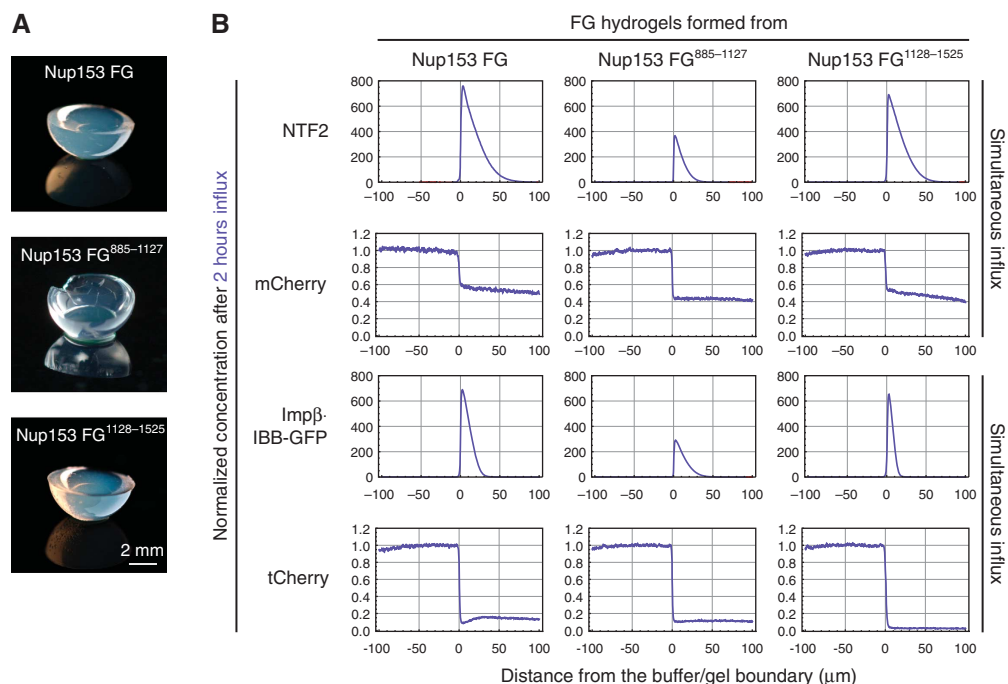


Figure 3 FG subdomains of *Xenopus tropicalis* Nup153 form highly selective hydrogels. (A) Photographs of indicated gels. (B) Permeability properties of Nup153-derived FG hydrogels were analysed as in Figure 2C (2 h time points).

domains (Ader *et al*, 2010; Yamada *et al*, 2010). The FG content of Nup358 is scattered over nine individual subdomains (Supplementary Figure S1), and it was striking to observe that all four tested individual subdomains (representing the longest and the most charged FG subdomains) as well as the combination of all nine FG subdomains formed hydrogels (Figure 1A). Moreover, the gel derived from the combined Nup358 FG domains excluded even our smallest inert permeation probe (mCherry) rather efficiently (Figure 1C), which points to an efficient formation of a small-meshed barrier.

Nup153 is asymmetrically localized to the nuclear side of NPCs (Sukegawa and Blobel, 1993). Its FG domain (Nup153⁸⁸⁵⁻¹⁵²⁵) comprises a total of 641 residues and 32 FG motifs. It can be divided into two parts of rather different amino-acid composition. Nup153¹¹²⁸⁻¹⁵²⁵ contains only 2.5% charged residues, while Nup153⁸⁸⁵⁻¹¹²⁷ contains 21% (Table I). Nevertheless, we observed that the complete Nup153 FG domain and both FG subdomains formed hydrogels (Figure 3A) that efficiently excluded the tetrameric Cherry marker and showed an NPC-like permeability (Figure 3B). These results suggest that the apparent anti-cohesion effect of the charged residues might be compensated by unusually hydrophobic FG motifs (such as FLFG or FIFG), but possibly also by the formation of salt bridges between acidic and basic side chains.

Synergy between the gel-forming domains of the Nup62·54·58 complex

The Nup62·54·58 subcomplex (Finlay *et al*, 1991; Guan *et al*, 1995) is localized in the central part of NPCs (Grote

et al, 1995). *Xenopus laevis* Nup62, Nup54 and Nup58 contain N-terminal FG domains, Nup58 in addition also C-terminal FG repeats. Nup54 and Nup58 further comprise FG-like domains that flank the FG domains; these resemble in amino-acid composition a canonical FG domain, but lack *bona fide* FG motifs (Figure 4A; Supplementary Figure S1). Nevertheless, we found by binding assays and peptide arrays that these FG-like domains interact with NTRs to a significant extend, possibly through alternative hydrophobic motifs (Supplementary Figure S3). We regard them therefore as further examples of FG-like domains.

The analysis of hydrogels, which include only the canonical Nup54 or Nup58 FG domains, revealed a surprisingly high permeability for and considerable non-specific binding of mCherry and tCherry (Figure 1C). Gels that combined each the FG and FG-like domains from either Nup54 or Nup58 showed a reduced but still persisting non-specific binding of inert probes (Figure 4B; Supplementary Figure S4). The Nup62 FG gel was already more selective and clearly suppressed entry of mCherry and tCherry, resulting in partition coefficients of 0.7 and 0.6, respectively.

As a next step, we fused FG and FG-like domains of all three Nups in tandem, expecting the corresponding composite gel to behave like an average of the three individual domains. We, however, observed a striking synergy between these domains. The fused domains now formed a gel that completely excluded tCherry and efficiently suppressed entry of mCherry (partition coefficient ≈ 0.2 ; Figure 4B). It is also remarkable that the exquisite barrier performance was lost when the FG-like domains of Nup54⁹⁵⁻¹³⁹ and Nup58⁷³⁻²⁵⁹ had been omitted from the fusion.

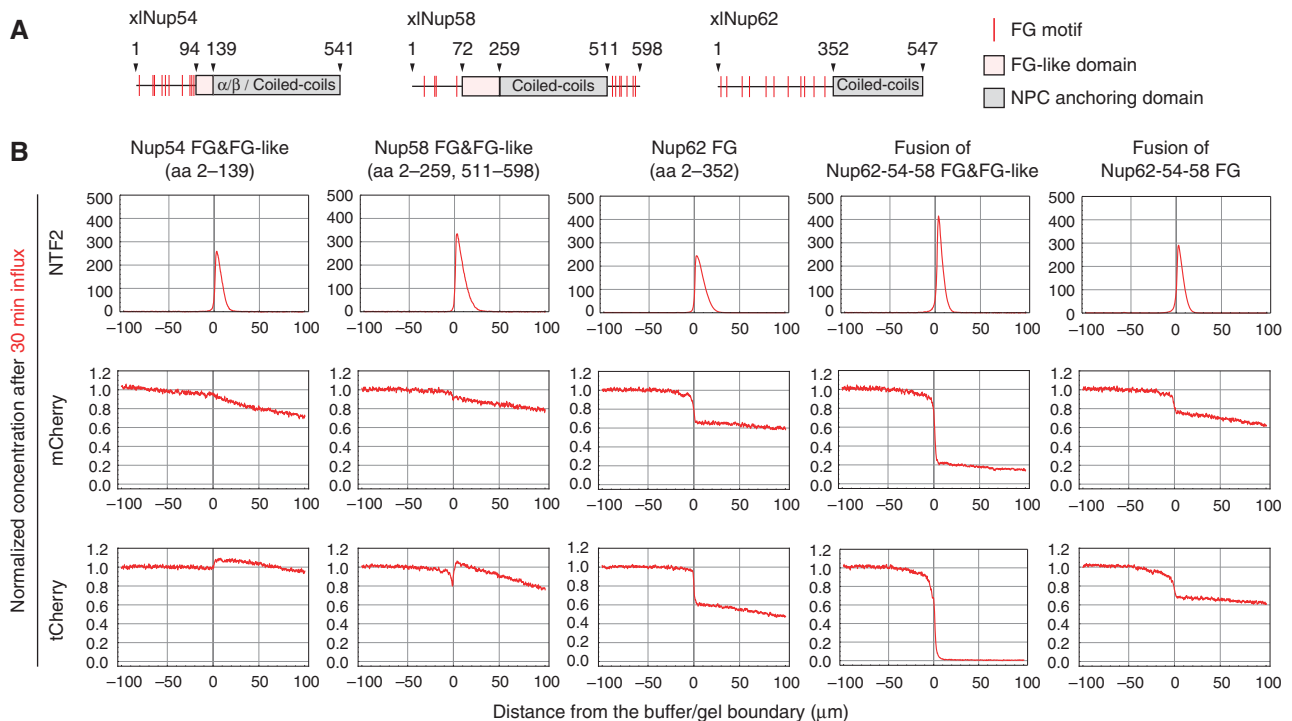


Figure 4 Permeability properties of hydrogels derived from the *Xenopus laevis* Nup62 complex. (A) Domain organizations of Nup54, Nup58 and Nup62. (B) Hydrogels obtained from indicated nucleoporin fragments or domain fusions were probed with NTF2, mCherry or tCherry as in Figure 1B (30 min time points). Please note that the Nup54 and Nup58 hydrogels here also include the FG-like domains, which had been omitted in Figure 1C.

A pure Nup98 FG hydrogel is too restrictive for passage of large NTRs

Nup98 shows by post-embedding immuno-EM a very central localization within the central translocation channel of the NPC (Krull *et al*, 2004). Thus, it would be ideally positioned to control passage through the pore, and indeed, Nup98 is essential for maintaining a functional permeability barrier in *Xenopus* NPCs (Hülsmann *et al*, 2012). It probably occurs in three copies per asymmetric unit, two being anchored through Nup96 to the Nup107–160 subcomplexes (Vasu *et al*, 2001; Hodel *et al*, 2002), and one associating with the Nup214·Nup88·Nup62 subcomplex (Griffis *et al*, 2003). *Xenopus* Nup98 has an N-terminal FG domain comprising 485 residues (Supplementary Figure S1) with an embedded GLEBS domain that interacts with the mRNA export mediator Gle2p/Rae1 (Prichard *et al*, 1999).

The Nup98 FG domain has the highest density of FG motives of all *Xenopus* FG domains, namely one motif per ≈ 10 residues (Table I). The derived Nup98 FG hydrogel appeared an ideally selective barrier when probed with NTF2 and mCherry (Figure 1B): It completely blocked entry of mCherry, but allowed an at least 100 000-fold faster influx of NTF2. Closer inspection revealed, however, that the extreme tightness towards inert probes had an unexpected side effect, namely that all tested importins and exportins bound only to the gel surface and failed to visibly penetrate into the gel (shown for Imp β ·cargo complexes in Figure 5C). Such over-tight barrier in authentic NPCs would impede NTR-

mediated nuclear transport of small proteins and even more so the transit of large (e.g., ribosome-sized) cargoes. We therefore considered several mechanisms that might confer a higher permeability to a Nup98 FG gel-based barrier.

A first possibility is that the local FG domain concentration of the *in vitro*-formed hydrogel is higher than in authentic NPCs, and so lowering the concentration should increase the permeability. The FG domains of, for example, scNsp1p or Nup214 form homogeneous gels over a wide range of concentrations (10–200 mg/ml). The Nup98 FG domain also forms a homogeneous gel at 200 mg/ml. When we attempted, however, to lower the concentration of the Nup98 FG domain, we observed a striking phase separation into a protein-rich and a protein-poor phase. The microscopic appearance of the resulting gels then resembled a ‘holey Swiss cheese’ (Figure 5A). It should be noted that shrinking of the gel drop was evident also for a starting concentration of 200 mg/ml, though in this case, shrinking reduced the volume of the entire gel drop and did not disintegrate the gel. The super-tight Nup98 gel therefore had a protein concentration probably exceeding 200 mg/ml.

The effect can be explained by the concept of a saturated FG hydrogel (Frey and Görlich, 2007), which assumes that all cohesive units of an FG domain can find sufficiently close binding partners only when their concentration exceeds a certain saturation limit. Undersaturated gels should contain a significant share of unpaired cohesive units and hence have a larger mesh size than the equivalent saturated gel. This

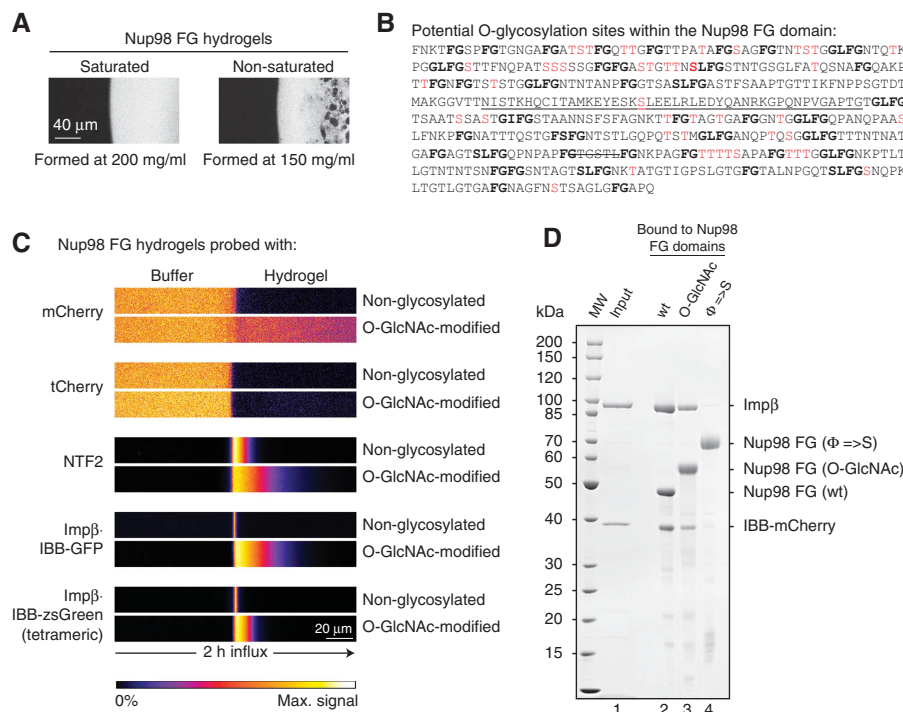


Figure 5 Analysis of Nup98 FG hydrogels. (A) The non-glycosylated Nup98 FG domain forms an inhomogeneous hydrogel at the concentrations below 200 mg/ml. Microscopic pictures illustrate the appearance of saturated and non-saturated Nup98 FG hydrogels. (B) Potential O-GlcNAc modification sites within the Nup98 FG domain were identified by mass spectrometry after enzymatic *in vitro* glycosylation. Modified Ser and Thr residues are shown in red, non-sequenced regions as strikethrough text, FG motifs in bold, the GLEBS domain is underlined. (C) Non-glycosylated or O-GlcNAc-modified Nup98 FG hydrogels were probed with indicated mobile species as described in Figure 1C (2 h time points). (D) The non-glycosylated and O-GlcNAc-modified Nup98 FG domains, as well as the Nup98 FG ($\Phi \Rightarrow S$) mutant were immobilized on Ni(II) Silica beads and incubated with a pre-formed Imp β ·IBB-mCherry complex. Bound fractions were analysed by SDS-PAGE and Coomassie staining. The $\Phi \Rightarrow S$ mutant, where all hydrophobic residues had been exchanged to serines, runs slower than expected from its mass.

state appears, however, instable in an undersaturated Nup98 gel. Here, it appears that the number of cohesive interactions is maximized by shrinking the gel volume until the saturation limit is reached. This shrinking then also leaves protein-poor areas behind (either by an increased buffer volume or as ‘holes in the cheese’). This effect qualifies the Nup98 FG domain as ‘highly cohesive’. The effect precluded analysing the permeability properties of a macroscopic, undersaturated Nup98 gel. It is well possible, however, that the anchoring of the domain to the rigid scaffold of an NPC would counteract such phase separation.

The Nup98 hydrogels respond to O-GlcNAc modifications

Another consideration is that native Nup98 is heavily modified by O-linked β -N-acetylglucosamines (O-GlcNAc; Powers *et al*, 1995), which are introduced by the O-GlcNAc transferase (OGT) that transfers GlcNAc moieties from UDP-GlcNAc to serines and threonines of numerous target proteins (Haltiwanger *et al*, 1990; Lubas and Hanover, 2000). To study the effects of this modification, we established a preparative method of enzymatically modifying the Nup98 FG domain. The reaction resulted in an electrophoretic size shift of ≈ 9 kDa (Figure 5D, lanes 2 and 3). Mass spectrometry revealed 46 potential modification sites, namely 29 threonines and 17 serines that occurred in clusters of up to 5 consecutively modified residues (Figure 5B). Otherwise, the modifications were distributed over the entire length of the FG domain. The *in vitro* reconstituted glycosylation reaction can be considered as a formal proof for Nup98 being an OGT substrate.

O-GlcNAc modification drastically changed the permeability properties of the Nup98 hydrogel. The glycosylated hydrogel allowed rapid entry and intragel diffusion not only of

NTF2, but also of larger NTR·cargo complexes, such as Imp β ·IBB-GFP (≈ 120 kDa) or an ≈ 480 kDa tetramerized Imp β ·IBB-zsGreen complex (Figure 5C). Concomitantly, the permeability towards mCherry increased. Nevertheless, the O-GlcNAc-modified Nup98 gel fully blocked entry of tCherry (Figure 5C). The combination of all these criteria qualifies this gel as the most selective of all the hydrogels derived from *Xenopus* FG domains.

Direct binding assays indicated that the O-GlcNAc modification slightly decreased the strength of the NTR·FG interaction (Figure 5D). Nevertheless, we observed that the O-GlcNAc-modified Nup98 gels absorbed NTRs far more efficiently than the non-modified Nup98 gel. This once again indicates that NTRs experience difficulties in breaking inter repeat contacts of the non-glycosylated gel and therefore enter such gel less efficiently.

The O-GlcNAc-modified Nup98 FG hydrogel reproduces sensitivity towards the NPC inhibitor WGA

Wheat germ agglutinin (WGA) is a tetravalent lectin recognizing GlcNAc moieties (Nagata and Burger, 1974). It binds O-GlcNAc-modified Nups (Finlay *et al*, 1987; Hanover *et al*, 1987; Holt *et al*, 1987) and blocks passage through vertebrate NPCs (Finlay *et al*, 1987). Initially, it was thought to be a selective inhibitor of facilitated translocation. Subsequent studies, however, revealed that the extent of inhibition does not depend on the mode of NPC passage, but on the size of the translocating species (Mohr *et al*, 2009). WGA blocks NPC passage of typical Imp β ·cargo complexes (mass > 100 kDa), but also strongly inhibits facilitated translocation of NTF2 or passive passage of GFP (mass ≈ 30 kDa).

If the glycosylated Nup98 gel would make up the selectivity filter of NPCs, then one would expect that the gel itself shows a similar sensitivity towards WGA. In line with this predic-

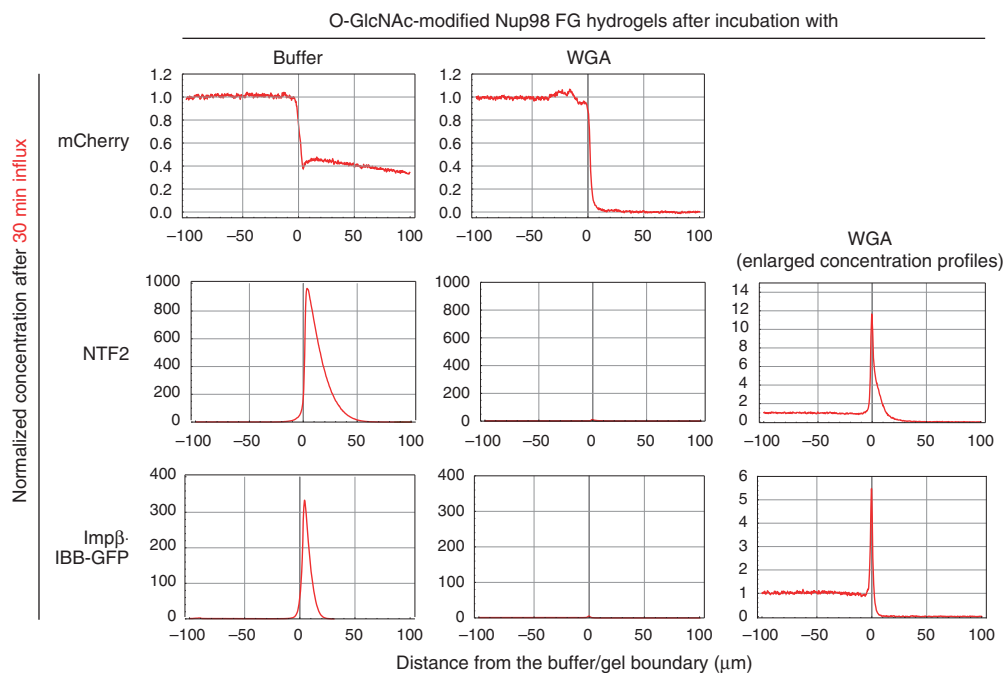


Figure 6 WGA inhibits passive diffusion and facilitated entry into an O-GlcNAc-modified Nup98 FG hydrogel. The gels were pre-incubated with either buffer (left column) or WGA and subsequently probed with mCherry, NTF2 and an Imp β ·cargo complex (30 min time points).

tion, we observed that pre-incubation of the gel with WGA essentially blocked influx of mCherry (Figure 6). NTF2 could still enter the WGA-treated gel, but at a rate that was at least 100-fold reduced as compared to the untreated one. The larger Imp β ·IBB-GFP complex completely failed to penetrate into the WGA-treated gel and displayed only a very weak residual binding to its surface. This reproduces the NPC inhibition by WGA and suggests that the *in vitro*-formed O-GlcNAc-modified Nup98 gel is indeed very similar to the authentic NPC barrier. In both cases, we assume that the tetravalent lectin introduces additional cross-links into the FG hydrogel that cannot be resolved by any NTR species.

Structural characterization of Nup98 FG hydrogels

As a next step, we analysed uniformly ^{13}C , ^{15}N -labelled variants of the Nup98 gel by several ssNMR methods (Andronesi *et al*, 2005). Through-space magnetization transfer (cross-polarization; CP) allows probing of very rigid regions that are stable for at least several milliseconds. Through-bond magnetization (Insensitive Nuclei Enhanced by Polarization Transfer; INEPT) detects highly mobile regions with motions in the nanoseconds regime. The two techniques are less sensitive for protein segments moving in a time frame of microseconds to milliseconds. However, this gap can be closed by direct excitation, which detects signals independently of mobility.

The previously characterized scNsp1 FG hydrogel yielded strong CP signals that can be attributed to the highly cohesive scNsp1 $^{1-175}$ FG subdomain (forming the rigid parts of the gel) as well as strong INEPT signals that predominantly stem from the non-cohesive and highly charged scNsp1 $^{274-601}$ FG subdomain (Ader *et al*, 2010; Figure 7A and B). Analysis of the non-glycosylated Nup98 gel revealed very strong CP signals and very low INEPT signals. This is consistent with our observation that this type of gel is so rigid that importin β -type NTRs fail to enter. The almost complete lack of INEPT-visible mobile elements further suggests that the Nup98 FG domain is cohesive along its entire sequence. This assumption is supported by two-dimensional ^{13}C , ^{13}C experiments (Figure 7C), indicating that all amino acid-specific cross-peaks detected by direct excitation also appear in the CP spectrum. It therefore appears that all NMR-resolved parts of the Nup98 FG domain reside in low mobility regions of the gel.

Based on these spectra, we conducted a qualitative analysis of secondary structure using secondary chemical-shift information (Ader *et al*, 2010). This analysis suggested that the rigid components of non-glycosylated Nup98 gel are not *per se* associated with the formation of β -strand structures as previously seen for the most rigid (NQ-rich amyloid-like) regions in scNsp1 FG hydrogel. This notion is based on the facts that the relevant cross-peaks in the Nup98 FG hydrogel are broader (Figure 7C, see below) and extend into spectral regions typically not associated with β -strands (Luca *et al*, 2001).

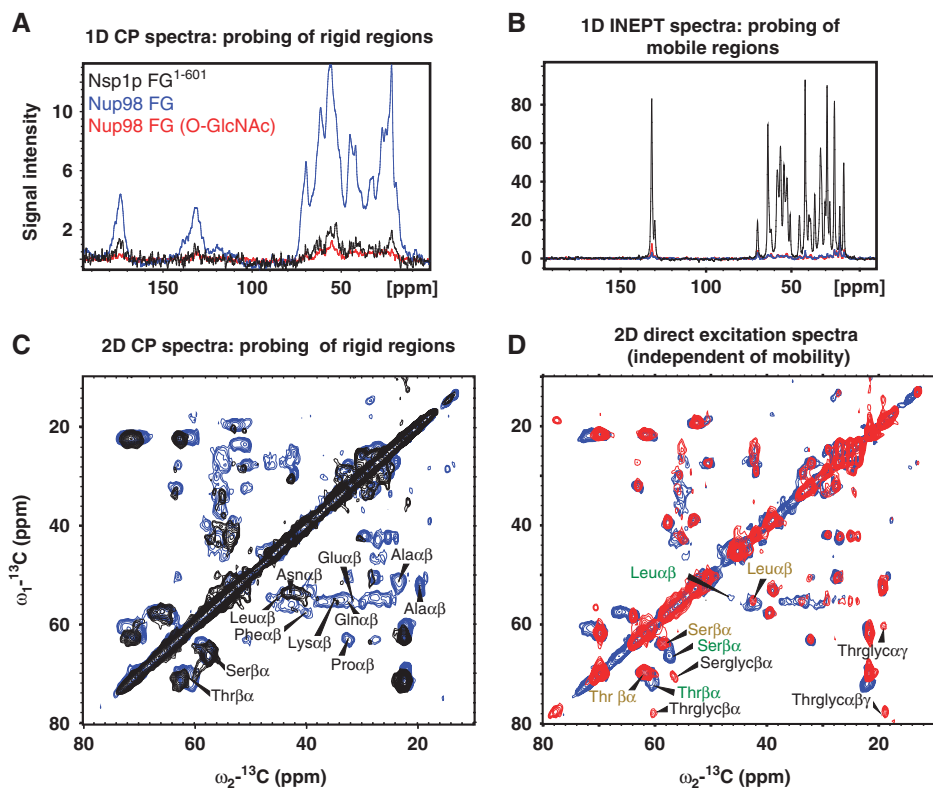


Figure 7 Solid-state NMR analysis of scNsp1- and Nup98-derived FG hydrogels. (A) 1D cross-polarization (CP) spectra probing very rigid parts of the scNsp1 FG hydrogel (black curve), a non-glycosylated Nup98 FG hydrogel (blue) and a O-GlcNAc-modified Nup98 gel (red). (B) INEPT spectra probing highly mobile regions of the same gels (colour coding as in A). (C) 2D CP spectra probing very rigid parts of the scNsp1 gel (black) and the non-glycosylated Nup98 FG hydrogel (blue). Indicated correlations reflect inter-atomic polarization transfer among aliphatic carbon positions (denoted by α - γ) for selected residue types. Resonance frequencies encode information about the identity of residues and their backbone conformations. (D) 2D direct excitation spectra comparing non-glycosylated (blue) and O-GlcNAc-modified (red) Nup98 FG hydrogels. Resonance peaks indicating β -strand conformation are labelled in green, random coil conformations are coloured in mustard yellow.

Upon glycosylation, CP signal intensities of the Nup98 gel dropped dramatically (Figure 7A), illustrating that the O-GlcNAc modification makes the gel less rigid. Interestingly, we observed only a tiny concomitant increase in the INEPT signal (Figure 7B), suggesting that the glycosylated gel was still largely devoid of fully mobile regions and that the O-GlcNAc-modified Nup98 FG domain remained cohesive along its entire sequence.

2D data sets of the glycosylated Nup98 gel could only be obtained using direct excitation, which omits the preparatory CP step and which is therefore rather insensitive towards protein mobility. The spectra then showed the expected appearance of signals specific for O-GlcNAc-modified threonines and serines (in Figure 7D annotated with 'glyc'). Their intensities are consistent with the degree of modification measured by mass spectrometry. The fact that these glycosylation-specific signals produced the strongest cross-correlations in 2D spectra following direct excitation suggests that the modifying groups do not just prevent intragel contacts. Instead, they appear to engage in novel interactions that limit their mobility to a microseconds to milliseconds regime that seems characteristic for the entire glycosylated Nup98 gel.

Surprisingly, correlations compatible with β -sheet arrangements (Figure 7D, labelled in green) were completely absent from the O-GlcNAc-modified Nup98 gel. Instead, we observed correlations (Figure 7D, mustard yellow) that are typically observed in unstructured protein loop regions (also known as random coil correlations; Luca *et al*, 2001). This is in striking contrast to the interchain β -sheet structures that dominate inter FG repeat contacts of the highly cohesive NQ-rich FG domains from the yeast *S. cerevisiae* (Ader *et al*, 2010). This points to a fully unanticipated conclusion, namely that FG hydrogels can assemble through different structural principles and yet acquire the same NPC-typical permeability.

Discussion

The NPC permeability barrier is a central module of the nuclear transport machinery. It suppresses uncontrolled intermixing of nuclear and cytoplasmic contents, but permits rapid passage of NTR-cargo complexes. Directed active nuclear transport requires the barrier to prevent a backflux of cargoes from their destination compartments. Furthermore, importin- and exportin-mediated transport cycles are driven by tightly coupled RanGTPase cycles, which, again, rely on the NPC barrier for retaining free RanGTP inside the nuclear compartment.

The principle of inter FG repeat cohesion is evolutionary conserved

We previously proposed the selective phase model to explain NPC barrier function (Ribbeck and Görlich, 2001). It assumes a non-covalent cross-linking of barrier-forming FG domains into a 3D sieve excluding large inert molecules, but allowing NTRs to transiently open adjacent meshes and thus to pass the barrier. If FG hydrogel formation was fundamental for nuclear transport selectivity, then one should expect evolutionary conservation of this principle. Indeed, it is now evident that not only yeast contains cohesive FG domains (Frey and Görlich, 2009; Yamada *et al*, 2010), but also *Xenopus*, that is, an organism separated by ≈ 1 billion years of evolution. We now tested 10 FG domains as well as

several FG-like domains from *Xenopus* and found them all proficient in hydrogel formation. Together, these domains account for $\approx 1/7$ of the so far attributable mass of the NPC proper. Considering that the *Xenopus* nucleoporins contain additional domains with predicted non-globular structure (e.g., in Pom121, Ndc1 or Nup88), this number might be even higher. We would assume that hydrogel structures within the NPC not only participate in the permeability barrier, but also function as an adaptive glue between certain NPC subcomplexes.

Composite hydrogels from neighbouring FG domains

We expect the territorial boundaries between individual FG domains to be blurred and FG domains with adjacent anchor points to intermix and to form composite gels. This will certainly apply to FG domains that originate from the same subcomplex, where the contour length of the domains (typically in the 100-nm range) by far exceeds the distance between the respective anchor points (which is presumably just a few nm). Our observations with the Nup62·54·58 subcomplex indicate that such FG domain mixing might be even functionally relevant, because here the composite gel comprising all gel-forming domains displayed a far better selectivity than any of the individual homotypic gels (Figure 4). Extending this, it appears well possible that other FG domains, which form individually only gels with poor exclusion of inert macromolecules (e.g., the Pom121 FG domain), might actually perform well in the context of an authentic NPC.

NPCs apparently contain several gel layers of distinct mesh sizes

Our data further suggest that FG hydrogel-containing regions prevail not only in the central channel, but also extend far to the NPC peripheries. Nup358, for example, contains large sequence stretches of high gel-forming propensity. A peptide contained within the gel-forming part was previously localized ≈ 70 nm in cytoplasmic direction from the NPC mid-plane (Walther *et al*, 2002). On the other side, Nup153 localizes far to the nuclear side and also contributes a substantial share of gel-forming FG domain mass. In between, we expect FG gels derived from Nups 214, 98, 62, 58 and 54, as well as from Pom121. The long distances between the farthest cytoplasmic and farthest nuclear gel-forming FG domain anchor points suggest that the permeation path across an NPC leads through stratified layers of gels that differ in composition and selectivity. Even within the central channel we cannot expect the barrier-forming gel to be fully homogeneous, because different anchor points and the fact that naturally occurring FG domains do not represent perfectly repeated sequences will impose a compositional bias. Our data further point to a coarser sieving at the periphery and strict sieving at the Nup98-dominated narrowest point of the central channel.

O-GlcNAc modification as a permeability modifier of FG hydrogel-based barriers

The permeability of NPCs needs to be balanced. Too loose barriers will favour intermixing of nuclear and cytoplasmic contents and deteriorate the RanGTP gradient, while too tight barriers might block passage of NTRs carrying large cargoes. It is tempting to assume that the yeast *S. cerevisiae* achieves

an optimal balance by combining extremely cohesive FG domains (such as those from scNup100p or scNup116p, which are related to NQ-rich amyloids) with non-cohesive ones that are typically highly charged. We now observed that *Xenopus* (and thus perhaps other metazoan species) can use an additional way of modifying their FG gel permeability, namely by extensive O-GlcNAc modifications of their most tightly interacting FG domains.

As exemplified for the Nup98 hydrogel, glycosylation makes the entire gel more dynamic (to a microseconds to milliseconds regime; Figure 7) and greatly favours the entry of large NTR·cargo complexes (Figure 5C). The attached sugar is very hydrophilic and so it probably improves the water solubility of the hydrogel and allows the gels to retain a higher content of water. Nup62 is another highly glycosylated Nup of *Xenopus* NPCs (Finlay *et al*, 1991), and we observed, also in this case, that the modification weakens inter FG repeat cohesion and favours entry of large NTRs into a formed gel (Supplementary Figure S5). The O-GlcNAc modification of Nup98 or Nup62 subcomplex might be beneficial already before an incorporation into NPCs by suppressing precipitation of these otherwise rather aggregation-prone molecules.

An interesting aspect is the reversibility of the O-GlcNAc modification (Gao *et al*, 2001). Cells might exploit this effect and regulate the permeability of their NPCs through changes in the activities of OGT and/or of the antagonistic glycosidase. Our preliminary data indicate that Nup98 from *Xenopus* eggs is O-GlcNAc modified to only 50% of the levels reached by excess of OGT, leaving indeed room for an upregulation as well as for a downregulation of the modification.

***Xenopus* and *S. cerevisiae* appear to prefer different modes of inter FG repeat cohesion**

The most cohesive *S. cerevisiae* FG repeat regions (from scNup100p, scNup116p or the scNsp1 N-terminus) resemble NQ-rich amyloids not only in sequence, but also by the occurrence of interchain β -sheets, which account for the most stable interactions at least within an scNsp1 FG hydrogel (Ader *et al*, 2010; Yamada *et al*, 2010; Halfmann *et al*, 2012). Such β -structures are less prevalent in a non-modified Nup98 FG hydrogel and entirely absent in the fully O-GlcNAc-modified gel (Figure 7D). It thus appears that the bulkiness of the sugars sterically excludes interchain β -sheets. The fact that the glycosylated Nup98 domain still forms a highly selective gel suggests that other intermolecular interactions dominate. One plausible structural element would be analogous to micelles, where hydrophobic residues of FG motifs aggregate to 'miniaturized hydrophobic cores' that are interconnected by hydrophilic and possibly glycosylated spacers. The observation that the Nup98 FG domain has a considerably larger proportion of hydrophobic residues than the NQ-rich yeast FG domains is consistent with this assumption. Taken together, it appears that there are at least two fundamentally different ways of organizing a functional NPC barrier.

Given these striking differences in gel structures, it is remarkable that the NQ-rich FG domains from scNup100p or scNup116p can functionally replace the Nup98 FG domain in reconstituted *Xenopus* NPCs and thus support facilitated passage of *Xenopus* NTRs (Hülsmann *et al*, 2012). Conversely, yeast NTRs can enter the glycosylated Nup98 FG hydrogel in a highly facilitated manner (Supplementary

Figure S6). This suggests that both types of inter FG repeat contacts become unstable when the engaged FG motifs are bound by a transiting NTR.

Why do vertebrates not rely on NQ-rich FG domains? One possible explanation is that such domains not only form reversible hydrogels, but also pose a risk of occasionally forming true amyloid fibres (Halfmann *et al*, 2012), which might then trigger pathogenic processes. The accumulated risk should be greater for long-lived vertebrates than for a unicellular, rapidly multiplying species.

Sequence requirements for a selective FG hydrogel

We found that a wide range of nucleoporin FG- and FG-like domains, which share hardly any sequence identity, is able to form hydrogels. This begs the questions of how diverse the sequence space of gel-forming modules actually can be and what sequence features are critical for a well-performing barrier.

A first requirement is certainly that the sequence is sufficiently hydrophobic to become self-interacting (cohesive). Indeed, NQ-rich FG domains and the Nup98 FG domain become non-cohesive when their hydrophobic residues are mutated to serines (Frey *et al*, 2006; Hülsmann *et al*, 2012). For conferring intermolecular interactions, these hydrophobic residues should, however, not be buried by intramolecular interactions, that is, the sequence must not adopt a globular fold. This criterion is probably easy to meet, as only a tiny fraction of random sequences can be expected to yield a globular domain.

Furthermore, heat-shock proteins or the protein degradation machinery must not misrecognize FG domains as molten globules or misfolded proteins. Indeed, typical Hsp70 recognition motifs are more hydrophobic than FG motifs (Rüdiger *et al*, 2000) and appear strongly underrepresented in FG domains. A maximized distance to HSP-recognition motifs could also explain why certain residues, such as Cys, Tyr, or Trp, are significantly underrepresented in FG domains as compared to globular domains.

In addition, the FG domains should bind NTRs, a property which is most efficiently conferred by FG motifs (Cushman *et al*, 2006). FG domains should, however, be selected against non-specific protein interactions that would deteriorate the selectivity of the barrier or even set seeding points for protein aggregation that could irreversibly plug the NPC. Given that accessible hydrophobic residues, which are typical for FG domains, are prone for causing non-selective interactions, this is a rather non-trivial criterion. It is met by as-yet undeciphered rules for the sequence context of FG motifs. We found, however, also instances where distinct FG domains 'passivate' each other. The FG domains of Nup54 or Nup58, for example, display a significant non-selective interaction with tCherry, which is fully suppressed in the presence of the Nup62 FG domain (compare Figures 1C and 4B; Supplementary Figure S4). The NQ-rich part of the scNsp1 FG domain also forms a gel with non-selective protein binding, and again, this is suppressed by other FG repeats, namely by the charged region of the same FG domain (Ader *et al*, 2010).

Finally and most importantly for facilitated NPC passage, FG hydrogels should assemble such that NTRs can locally dissolve the meshes. The precise mechanism of this process is still fully obscure. So far, we only have evidence that it

happens, namely when NTR 'melt' into gels that are fully inaccessible for inert molecules of the same size.

Materials and methods

DNA constructs, protein expression and purification

Xenopus FG and FG-like domains were predicted *in silico* from ESTs and the genome of *X. tropicalis*. The indicated protein sequences and domain boundaries refer to the following accession numbers (available from DDBJ/EMBL/GenBank): xNup214: AJ243889; xtNup153: JX993585; xNup62: BC106600; xNup54: JX993586; xNup58: BC090209; xNup50: BC077201; xtNup98: JX136847; xICG1 (also known as nucleoporin-like protein 2): Q5XGN1; xIPOM121: AY676874; xtNup358: XP_002937704. Coding sequences were subcloned from IMAGE clones or cDNA into bacterial expression vectors (Supplementary Figure S1; Supplementary Table S1). All proteins used were expressed in *E. coli*, FG domains in the strain KY2266 (Kanemori *et al*, 1997) and other proteins in BLR. The production of the following proteins has been described before: transportin, NTF2 (Ribbeck and Görlich, 2001), CRM1, RanQ69L¹⁻¹⁸⁰, PKI-NES-GFP (Güttler *et al*, 2010), mCherry (Frey and Görlich, 2009). For all other proteins, new bacterial expression vectors were created (Supplementary Table S1).

The tetrameric Cherry was derived from mCherry by restoring the tetramerizing interface of DsRed (Wall *et al*, 2000).

All NTRs, transport substrates and OGT were purified by native Ni(II) chelate chromatography, Tev-cleavable tags were cleaved with Tev protease (with exception of His10-GFP-Tev-Imp α). Proteins were further purified by gel filtration on a Superdex 200 column equilibrated in 50 mM Tris-HCl pH 7.5, 200 mM NaCl, 2 mM DTT, and snap-frozen after adding 250 mM sucrose.

FG domains were essentially purified as described previously for the scNsp1 FG domain (Frey and Görlich, 2007). In brief, Ni-chelate chromatography was performed in 6 M Guanidinium hydrochloride. FG domains were then rebuffed to 20% acetonitrile + 0.08% TFA and lyophilized.

In vitro glycosylation

Ni(II) chelate beads were loaded with FG domains from bacterial lysates, washed with GuHCl buffer (50 mM Tris-HCl pH 7.5, 6 M guanidinium hydrochloride, 2 mM DTT), and equilibrated in OGT buffer (50 mM Tris-HCl pH 7.5, 200 mM NaCl, 20 mM MgCl₂, 2 mM DTT, 1% Tween-20). The beads were then resuspended in 20 volumes of 5 μ M OGT and 1 mM UDP-GlcNAc (Sigma-Aldrich U4375) and rotated for 16 h at room temperature. Beads were subsequently washed with OGT buffer, and GuHCl buffer and finally eluted with 0.5 M imidazole/HCl pH 7.5, 6 M guanidinium hydrochloride, 2 mM DTT. Eluted proteins were buffer exchanged on a C18 column to 20% acetonitrile + 0.08% TFA and lyophilized.

FG hydrogel formation

Lyophilized FG domains were resuspended at 200 mg/ml in a buffer (see below). Gel formation was allowed for 16 h at room temperature in a humidified chamber. Subsequently, the hydrogels were equilibrated in assay buffer (20 mM Tris pH 7.5, 130 mM NaCl, 2 mM MgCl₂) for 16 h at room temperature.

All FG domains studied here formed gels in a physiological buffer, however, the handling was far easier when gelation was retarded by using 0.2% TFA/0.5–2 M Guanidinium HCl as a resuspension buffer. All gels used in this study were formed under these conditions. To make the gels visible by fluorescence microscopy, they had been spiked with 0.2 μ M of Atto647N-labelled FG repeats.

Hydrogel permeation assays

Hydrogel permeation assays were performed as described (Frey and Görlich, 2009) using a Leica SP5 confocal laser-scanning microscope equipped with a 63 \times glycerol immersion objective.

NTRs and NTR-cargo complexes were used in assay buffer at a concentration of 1.5 μ M (referring to monomeric substrates), while inert substances were used at 3 μ M concentration.

For WGA-inhibition experiments, glycosylated Nup98 FG hydrogels were pre-incubated with 0.5 mg/ml WGA (Lectin from *Triticum vulgare*, Sigma-Aldrich L0390). Influx assays were also supplemented with 0.1 mg/ml WGA.

Each permeation assay was reproduced at least in six independent experiments.

Binding assays

Binding assays were carried out in 50 mM Tris-HCl pH 7.5, 200 mM NaCl, 2 mM DTT. In all, 15 μ l Ni(II) chelate beads were loaded with 0.5 nmol of either the non-modified Nup98 FG domain, or the O-GlcNAc-modified Nup98 FG domain, or the Nup98 FG $\Phi \Rightarrow$ S mutant. Washed beads were rotated for 45 min with 100 μ l Imp β -IBB-mCherry complex (2 μ M), which had been pre-formed and pre-purified on a Superdex 200 column. Beads were washed again. Bound proteins were eluted with SDS/imidazole and analysed by SDS-PAGE followed by Coomassie staining.

Solid-state NMR

Isotope-labelled, rich medium (110601402 *E. coli*-OD2 CN; Silantes, Mering, Germany) was used to produce the ¹³C- and ¹⁵N-double-labelled Nup98 FG domain. Purification and glycosylation of labelled protein was as described above. For gel formation, however, water was replaced by D₂O and gels were dialyzed against 200 mM Potassium phosphate buffer (pH 7.5) before analysis.

ssNMR experiments were conducted using 4 and 3.2 mm triple-resonance (¹H, ¹³C, ¹⁵N) probeheads at static magnetic fields of 11.7 T and 16.4 T (Bruker Biospin). Through-space transfer experiments were performed at 10.92 kHz magic angle spinning and 295 K. Typical proton field strengths for 90° pulses and SPINAL64 (Fung *et al*, 2000) decoupling ranged between 70 and 83 kHz. (¹³C, ¹⁵N) correlation spectra (Figure 7D) were obtained using proton-driven spin diffusion schemes under MIRROR conditions (Scholz *et al*, 2008) employing mixing times of 40 ms. In the case of 2D ssNMR spectroscopy after direct excitation, mixing times were set to 20 ms (Nup98 FG) and 200 ms (O-GlcNAc-Nup98 FG). ¹³C magnetization was produced using CP (contact times of 0.5 and 0.6 ms) or direct excitation using 90° ¹³C pulses at 50 kHz r.f. field strength. Through-bond transfer experiments were performed at 10.92 kHz magic angle spinning and 295 K using an INEPT-TOBSY scheme (Andronesi *et al*, 2005). A TOBSY (Baldus and Meier, 1996) mixing time of 6.6 ms and 10 kHz GARP (Shaka *et al*, 1985) decoupling were employed.

Mass spectrometric mapping of O-GlcNAc modified sites

The enzymatically glycosylated Nup98 FG domains were dissolved at 2 mg/ml in 2 M Urea, 50 mM Tris-HCl pH 7.5, 2 mM DTT and digested with 0.1 mg/ml chymotrypsin for 16 h at 25°C. Peptides were desalted on a C18 matrix and subjected to β -elimination (2 h at 50°C and pH 12), which converts a modified serine to an α -amino propenoic acid derivative and a modified threonine to an α -amino butenoic acid derivative (Wells *et al*, 2002). The resulting peptides were analysed without further chemical modifications under standard conditions with an LTQ Orbitrap XL equipped with Agilent nano LC System. Obtained spectra were analysed with Mascot 2.2 and searched for unmodified peptides and peptides containing the appropriate modifications. The non-modified FG domain was included as a negative control to sort out potentially false-positive glycosylation sites.

DDBJ/EMBL/GenBank nucleotide sequence accession numbers

The accession numbers are xtNup153: JX993585 and xNup54: JX993586.

Supplementary data

Supplementary data are available at *The EMBO Journal* Online (<http://www.embojournal.org>).

Acknowledgements

We wish to thank Jürgen Schünemann and Uwe Pleßmann for excellent technical support; Koray Kirli for the pKK vectors; Maarten Fornerod for a xNup214 clone; Irene Böttcher-Gajewski for help in photography; Jennifer Seefeldt for critical reading of the manuscript; and the Max-Planck-Gesellschaft for financial support. The ssNMR work was supported by the Netherlands Organization for Scientific Research (VICI grant 700.10.443 to MB)

and by the European Community's Seventh Framework Program FP7/2007–2013 under grant agreement no. 211800.

Author contributions: AAL conceived, performed and analysed experiments, prepared figures and edited the manuscript; SG performed and analysed ssNMR experiments; SF generated tCherry and supplied reagents; BBH generated and validated initial *Xenopus* Nup constructs; HU led mass spectrometric analysis; MB led ssNMR

analysis; DG supervised the project, conceived and analysed experiments and wrote the manuscript.

Conflict of interest

The authors declare that they have no conflict of interest.

References

- Ader C, Frey S, Maas W, Schmidt HB, Görlich D, Baldus M (2010) Amyloid-like interactions within nucleoporin FG hydrogels. *Proc Natl Acad Sci USA* **107**: 6281–6285
- Andronesi OC, Becker S, Seidel K, Heise H, Young HS, Baldus M (2005) Determination of membrane protein structure and dynamics by magic-angle-spinning solid-state NMR spectroscopy. *J Am Chem Soc* **127**: 12965–12974
- Balbirnie M, Grothe R, Eisenberg DS (2001) An amyloid-forming peptide from the yeast prion Sup35 reveals a dehydrated beta-sheet structure for amyloid. *Proc Natl Acad Sci USA* **98**: 2375–2380
- Baldus M, Meier BH (1996) Total correlation spectroscopy in the solid state. The use of scalar couplings to determine the through-bond connectivity. *J Magn Reson A* **121**: 65–69
- Bastos R, Ribas de Pouplana L, Enarson M, Bodoor K, Burke B (1997) Nup84, a novel nucleoporin that is associated with CAN/Nup214 on the cytoplasmic face of the nuclear pore complex. *J Cell Biol* **137**: 989–1000
- Bayliss R, Ribbeck K, Akin D, Kent HM, Feldherr CM, Görlich D, Stewart M (1999) Interaction between NTF2 and xFxFG-containing nucleoporins is required to mediate nuclear import of RanGDP. *J Mol Biol* **293**: 579–593
- Bernard R, Engelsma D, Sanderson H, Pickersgill H, Fornerod M (2006) Nup214-Nup88 nucleoporin subcomplex is required for CRM1-mediated 60 S preribosomal nuclear export. *J Biol Chem* **281**: 19378–19386
- Bernard R, van der Velde H, Fornerod M, Pickersgill H (2004) Nup358/RanBP2 attaches to the nuclear pore complex via association with Nup88 and Nup214/CAN and plays a supporting role in CRM1-mediated nuclear protein export. *Mol Cell Biol* **24**: 2373–2384
- Brohawn SG, Partridge JR, Whittle JR, Schwartz TU (2009) The nuclear pore complex has entered the atomic age. *Structure* **17**: 1156–1168
- Bullock TL, Clarkson WD, Kent HM, Stewart M (1996) The 1.6 angstroms resolution crystal structure of nuclear transport factor 2 (NTF2). *J Mol Biol* **260**: 422–431
- Chi NC, Adam EJ, Adam SA (1995) Sequence and characterization of cytoplasmic nuclear protein import factor p97. *J Cell Biol* **130**: 265–274
- Cushman I, Palzkill T, Moore MS (2006) Using peptide arrays to define nuclear carrier binding sites on nucleoporins. *Methods* **39**: 329–341
- Eanes ED, Glenner GG (1968) X-ray diffraction studies on amyloid filaments. *J Histochem Cytochem* **16**: 673–677
- Englmeier L, Olivo JC, Mattaj IW (1999) Receptor-mediated substrate translocation through the nuclear pore complex without nucleotide triphosphate hydrolysis. *Curr Biol* **9**: 30–41
- Fauchere JL, Pliska V (1983) Hydrophobic parameters pi of amino acid side chains from the partitioning of N-acetyl-amino-acid amides. *Eur J Med Chem* **18**: 369–375
- Finlay DR, Meier E, Bradley P, Horecka J, Forbes DJ (1991) A complex of nuclear pore proteins required for pore function. *J Cell Biol* **114**: 169–183
- Finlay DR, Newmeyer DD, Price TM, Forbes DJ (1987) Inhibition of in vitro nuclear transport by a lectin that binds to nuclear pores. *J Cell Biol* **104**: 189–200
- Fornerod M, van Deursen J, van Baal S, Reynolds A, Davis D, Murti KG, Franssen J, Grosveld G (1997) The human homologue of yeast CRM1 is in a dynamic subcomplex with CAN/Nup214 and a novel nuclear pore component Nup88. *EMBO J* **16**: 807–816
- Frey S, Görlich D (2009) FG/FxFG as well as GLFG repeats form a selective permeability barrier with self-healing properties. *EMBO J* **28**: 2554–2567
- Frey S, Görlich D (2007) A saturated FG-repeat hydrogel can reproduce the permeability properties of nuclear pore complexes. *Cell* **130**: 512–523
- Frey S, Richter RP, Görlich D (2006) FG-rich repeats of nuclear pore proteins form a three-dimensional meshwork with hydrogel-like properties. *Science* **314**: 815–817
- Fried H, Kutay U (2003) Nucleocytoplasmic transport: taking an inventory. *Cell Mol Life Sci* **60**: 1659–1688
- Fung BM, Khitritin AK, Ermolaev K (2000) An improved broadband decoupling sequence for liquid crystals and solids. *J Magn Reson* **142**: 97–101
- Gao Y, Wells L, Comer FI, Parker GJ, Hart GW (2001) Dynamic O-glycosylation of nuclear and cytosolic proteins: cloning and characterization of a neutral, cytosolic beta-N-acetylglucosaminidase from human brain. *J Biol Chem* **276**: 9838–9845
- Görlich D, Kostka S, Kraft R, Dingwall C, Laskey RA, Hartmann E, Prehn S (1995) Two different subunits of importin cooperate to recognize nuclear localization signals and bind them to the nuclear envelope. *Curr Biol* **5**: 383–392
- Görlich D, Pante N, Kutay U, Aebi U, Bischoff FR (1996) Identification of different roles for RanGDP and RanGTP in nuclear protein import. *EMBO J* **15**: 5584–5594
- Görlich D, Seewald MJ, Ribbeck K (2003) Characterization of Ran-driven cargo transport and the RanGTPase system by kinetic measurements and computer simulation. *EMBO J* **22**: 1088–1100
- Griffis ER, Xu S, Powers MA (2003) Nup98 localizes to both nuclear and cytoplasmic sides of the nuclear pore and binds to two distinct nucleoporin subcomplexes. *Mol Biol Cell* **14**: 600–610
- Grote M, Kubitschek U, Reichelt R, Peters R (1995) Mapping of nucleoporins to the center of the nuclear pore complex by post-embedding immunogold electron microscopy. *J Cell Sci* **108**: 2963–2972
- Guan T, Muller S, Klier G, Pante N, Blevitt JM, Haner M, Paschal B, Aebi U, Gerace L (1995) Structural analysis of the p62 complex, an assembly of O-linked glycoproteins that localizes near the central gated channel of the nuclear pore complex. *Mol Biol Cell* **6**: 1591–1603
- Güttler T, Görlich D (2011) Ran-dependent nuclear export mediators: a structural perspective. *EMBO J* **30**: 3457–3474
- Güttler T, Madl T, Neumann P, Deichsel D, Corsini L, Monecke T, Ficner R, Sattler M, Görlich D (2010) NES consensus redefined by structures of PKI-type and Rev-type nuclear export signals bound to CRM1. *Nat Struct Mol Biol* **17**: 1367–1376
- Halfmann R, Wright J, Alberti S, Lindquist S, Rexach M (2012) Prion formation by a yeast GLFG nucleoporin. *Prion* **6**: 391–399
- Haltiwanger RS, Holt GD, Hart GW (1990) Enzymatic addition of O-GlcNAc to nuclear and cytoplasmic proteins. Identification of a uridine diphospho-N-acetylglucosamine:peptide beta-N-acetylglucosaminyltransferase. *J Biol Chem* **265**: 2563–2568
- Hanover JA, Cohen CK, Willingham MC, Park MK (1987) O-linked N-acetylglucosamine is attached to proteins of the nuclear pore. Evidence for cytoplasmic and nucleoplasmic glycoproteins. *J Biol Chem* **262**: 9887–9894
- Hetzler MW, Wente SR (2009) Border control at the nucleus: biogenesis and organization of the nuclear membrane and pore complexes. *Dev Cell* **17**: 606–616
- Hodel AE, Hodel MR, Griffis ER, Hennig KA, Ratner GA, Xu S, Powers MA (2002) The three-dimensional structure of the autoproteolytic, nuclear pore-targeting domain of the human nucleoporin Nup98. *Mol Cell* **10**: 347–358
- Holt GD, Snow CM, Senior A, Haltiwanger RS, Gerace L, Hart GW (1987) Nuclear pore complex glycoproteins contain cytoplasmically disposed O-linked N-acetylglucosamine. *J Cell Biol* **104**: 1157–1164
- Hülsmann BB, Labokha AA, Görlich D (2012) The permeability of reconstituted nuclear pores provides direct evidence for the selective phase model. *Cell* **150**: 738–751

- Hurt EC (1988) A novel nucleoskeletal-like protein located at the nuclear periphery is required for the life cycle of *Saccharomyces cerevisiae*. *EMBO J* **7**: 4323–4434
- Hutten S, Kehlenbach RH (2006) Nup214 is required for CRM1-dependent nuclear protein export in vivo. *Mol Cell Biol* **26**: 6772–6785
- Imamoto N, Shimamoto T, Kose S, Takao T, Tachibana T, Matsubae M, Sekimoto T, Shimonishi Y, Yoneda Y (1995) The nuclear pore-targeting complex binds to nuclear pores after association with a karyophile. *FEBS Lett* **368**: 415–419
- Iovine MK, Watkins JL, Wentz SR (1995) The GLFG repetitive region of the nucleoporin Nup116p interacts with Kap95p, an essential yeast nuclear import factor. *J Cell Biol* **131**: 1699–1713
- Izaurralde E, Kutay U, von Kobbe C, Mattaj IW, Görlich D (1997) The asymmetric distribution of the constituents of the Ran system is essential for transport into and out of the nucleus. *EMBO J* **16**: 6535–6547
- Kanemori M, Nishihara K, Yanagi H, Yura T (1997) Synergistic roles of HslVU and other ATP-dependent proteases in controlling in vivo turnover of sigma32 and abnormal proteins in *Escherichia coli*. *J Bacteriol* **179**: 7219–7225
- Kraemer D, Wozniak RW, Blobel G, Radu A (1994) The human CAN protein, a putative oncogene product associated with myeloid leukemogenesis, is a nuclear pore complex protein that faces the cytoplasm. *Proc Natl Acad Sci USA* **91**: 1519–1523
- Krull S, Thyberg J, Björkroth B, Rackwitz HR, Cordes VC (2004) Nucleoporins as components of the nuclear pore complex core structure and Tpr as the architectural element of the nuclear basket. *Mol Biol Cell* **15**: 4261–4277
- Kubitscheck U, Grunwald D, Hoekstra A, Rohleder D, Kues T, Siebrasse JP, Peters R (2005) Nuclear transport of single molecules: dwell times at the nuclear pore complex. *J Cell Biol* **168**: 233–243
- Kustanovich T, Rabin Y (2004) Metastable network model of protein transport through nuclear pores. *Biophys J* **86**: 2008–2016
- Lubas WA, Hanover JA (2000) Functional expression of O-linked GlcNAc transferase. Domain structure and substrate specificity. *J Biol Chem* **275**: 10983–10988
- Luca S, Filippov DV, van Boom JH, Oschkinat H, de Groot HJM, Baldus M (2001) Secondary chemical shifts in immobilized peptides and membrane proteins: a qualitative basis for structure refinement under magic angle spinning. *J Biomol. NMR* **20**: 325–331
- Milles S, Lemke EA (2011) Single molecule study of the intrinsically disordered FG-repeat nucleoporin 153. *Biophys J* **101**: 1710–1719
- Mohr D, Frey S, Fischer T, Güttler T, Görlich D (2009) Characterisation of the passive permeability barrier of nuclear pore complexes. *EMBO J* **28**: 2541–2553
- Morrison J, Yang JC, Stewart M, Neuhaus D (2003) Solution NMR study of the interaction between NTF2 and nucleoporin FxFG repeats. *J Mol Biol* **333**: 587–603
- Nagata Y, Burger MM (1974) Wheat germ agglutinin. Molecular characteristics and specificity for sugar binding. *J Biol Chem* **249**: 3116–3122
- Onischenko EA, Gubanov NV, Kiseleva EV, Hallberg E (2005) Cdk1 and okadaic acid-sensitive phosphatases control assembly of nuclear pore complexes in *Drosophila* embryos. *Mol Biol Cell* **16**: 5152–5162
- Patel SS, Belmont BJ, Sante JM, Rexach MF (2007) Natively unfolded nucleoporins gate protein diffusion across the nuclear pore complex. *Cell* **129**: 83–96
- Petri M, Frey S, Menzel A, Görlich D, Techert S (2012) Structural characterization of nanoscale meshworks within a nucleoporin FG hydrogel. *Biomacromolecules* **13**: 1882–1889
- Powers MA, Macaulay C, Masiarz FR, Forbes DJ (1995) Reconstituted nuclei depleted of a vertebrate GLFG nuclear pore protein, p97, import but are defective in nuclear growth and replication. *J Cell Biol* **128**: 721–736
- Pritchard CE, Fornerod M, Kasper LH, van Deursen JM (1999) RAE1 is a shuttling mRNA export factor that binds to a GLEBS-like NUP98 motif at the nuclear pore complex through multiple domains. *J Cell Biol* **145**: 237–254
- Rexach M, Blobel G (1995) Protein import into nuclei: association and dissociation reactions involving transport substrate, transport factors, and nucleoporins. *Cell* **83**: 683–692
- Ribbeck K, Görlich D (2001) Kinetic analysis of translocation through nuclear pore complexes. *EMBO J* **20**: 1320–1330
- Ribbeck K, Kutay U, Paraskeva E, Görlich D (1999) The translocation of transport-cargo complexes through nuclear pores is independent of both Ran and energy. *Curr Biol* **9**: 47–50
- Ribbeck K, Lipowsky G, Kent HM, Stewart M, Görlich D (1998) NTF2 mediates nuclear import of Ran. *EMBO J* **17**: 6587–6598
- Rout MP, Aitchison JD, Magnasco MO, Chait BT (2003) Virtual gating and nuclear transport: the hole picture. *Trends Cell Biol* **13**: 622–628
- Rüdiger S, Mayer MP, Schneider-Mergener J, Bukau B (2000) Modulation of substrate specificity of the DnaK chaperone by alteration of a hydrophobic arch. *J Mol Biol* **304**: 245–251
- Scholz I, Huber M, Manolikas T, Meier BH, Ernst M (2008) MIRROR recoupling and its application to spin diffusion under fast magic-angle spinning. *Chem Phys Lett* **460**: 278–283
- Schwoebel ED, Talcott B, Cushman I, Moore MS (1998) Ran-dependent signal-mediated nuclear import does not require GTP hydrolysis by Ran. *J Biol Chem* **273**: 35170–35175
- Shaka AJ, Barker PB, Freeman R (1985) Computer-optimized decoupling scheme for wideband applications and low-level operation. *J Magn Reson* **64**: 547–552
- Shaner N, Campbell R, Steinbach P, Giepmans B, Palmer A, Tsien R (2004) Improved monomeric red, orange and yellow fluorescent proteins derived from *Drosophila* sp. red fluorescent protein. *Nat Biotechnol* **22**: 1567–1572
- Strawn LA, Shen T, Shulga N, Goldfarb DS, Wentz SR (2004) Minimal nuclear pore complexes define FG repeat domains essential for transport. *Nat Cell Biol* **6**: 197–206
- Sukegawa J, Blobel G (1993) A nuclear pore complex protein that contains zinc finger motifs, binds DNA, and faces the nucleoplasm. *Cell* **72**: 29–38
- Vasu S, Shah S, Orjalo A, Park M, Fischer WH, Forbes DJ (2001) Novel vertebrate nucleoporins Nup133 and Nup160 play a role in mRNA export. *J Cell Biol* **155**: 339–354
- von Moeller H, Basquin C, Conti E (2009) The mRNA export protein DBP5 binds RNA and the cytoplasmic nucleoporin NUP214 in a mutually exclusive manner. *Nat Struct Mol Biol* **16**: 247–254
- Wall MA, Socolich M, Ranganathan R (2000) The structural basis for red fluorescence in the tetrameric GFP homolog DsRed. *Nat Struct Biol* **7**: 1133–1138
- Walther TC, Pickersgill HS, Cordes VC, Goldberg MW, Allen TD, Mattaj IW, Fornerod M (2002) The cytoplasmic filaments of the nuclear pore complex are dispensable for selective nuclear protein import. *J Cell Biol* **158**: 63–77
- Weirich CS, Erzberger JP, Berger JM, Weis K (2004) The N-terminal domain of Nup159 forms a beta-propeller that functions in mRNA export by tethering the helicase Dbp5 to the nuclear pore. *Mol Cell* **16**: 749–760
- Wells L, Vosseller K, Cole RN, Cronshaw JM, Matunis MJ, Hart GW (2002) Mapping sites of O-GlcNAc modification using affinity tags for serine and threonine post-translational modifications. *Mol Cell Proteomics* **1**: 791–804
- Yamada J, Phillips JL, Patel S, Goldfien G, Calestagne-Morelli A, Huang H, Reza R, Acheson J, Krishnan VV, Newsam S, Gopinathan A, Lau EY, Colvin ME, Uversky VN, Rexach MF (2010) A bimodal distribution of two distinct categories of intrinsically disordered structures with separate functions in FG nucleoporins. *Mol Cell Proteomics* **9**: 2205–2224
- Yang W, Gelles J, Musser SM (2004) Imaging of single-molecule translocation through nuclear pore complexes. *Proc Natl Acad Sci USA* **101**: 12887–12892

